

Steric limitations in associative substitution reactions of $\text{Os}_3(\text{CO})_9(\mu\text{-C}_6\text{H}_4\text{Ph})$

Anthony J. Poë^{a,*}, David H. Farrar^{a,*}, Ravindranath Ramachandran^a, Consuelo Moreno^b

^a Lash Miller Chemical Laboratories, University of Toronto, 80 St. George Street, Toronto, Ont., M5S 3H6, Canada

^b Departamento de Química Inorgánica, Universidad Autónoma de Madrid, Cantoblanco, 28049-Madrid, Spain

Received 20 March 1997; accepted 9 June 1997

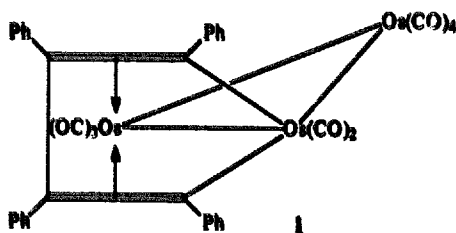
Abstract

Reactions of the cluster $\text{Os}_3(\text{CO})_9(\mu\text{-C}_6\text{H}_4\text{Ph})$ (**1**) with a large number of smaller P-donor nucleophiles (Tolman cone angle $\theta \leq 143^\circ$) proceed rapidly in heptane at room temperature via associative adduct formation to form the monosubstituted products. However, reactions with several larger P-donor nucleophiles ($\theta \geq 145^\circ$) in heptane at room temperature yield, in a single observable bimolecular step, a mixture of mononuclear and dinuclear products and it is therefore not possible to synthesize the monosubstituted clusters directly with these larger ligands. Crystallographic structures of $\text{Os}_3(\text{CO})_8(\text{etpb})(\mu\text{-C}_6\text{H}_4\text{Ph}) \cdot (\text{CH}_3\text{OH})$ (**2etpb**) (etpb = $\text{P}(\text{OCH}_2)_2\text{CEt}$) and $\text{Os}_3(\text{CO})_8(\text{P}(\text{OPh})_3)(\mu\text{-C}_6\text{H}_4\text{Ph}) \cdot (\text{C}_6\text{H}_6)$ (**2P(OPh)_3**) have been determined and show that the substituent has displaced a CO ligand from the $\text{Os}(\text{CO})_4$ moiety in **1**. © 1998 Elsevier Science S.A. All rights reserved.

Keywords: Osmacyclopentadiene complexes; Carbonyl complexes; Cluster complexes; P-donor substituents

1. Introduction

The cluster $\text{Os}_3(\text{CO})_9(\mu\text{-C}_6\text{H}_4\text{Ph})$ (**1**) contains an osmacyclopentadiene ligand that coordinates through the two conjugated $\text{C}=\text{C}$ bonds to one of the other Os atoms [1].



It is one of the products formed during the series of reactions beginning with $\text{Os}_3(\text{CO})_{12}$ and C_2Ph_2 [2], and reaction with a further molecule of C_2Ph_2 after dissociation of a CO ligand from **1** leads eventually to the oligomer C_6Ph_6 [3]. In this respect **1** exemplifies, in both its formation and its reactions, the way in which C–C coupling can be facilitated by metal carbonyl clusters [2,4]. Although this cluster has been known for many years no substituted derivatives have yet been fully

characterized. This could be because of the ease with which this Os_3 cluster undergoes fragmentation in spite of its presumably strong Os–Os bonds [5]. Reaction with CO proceeds smoothly between 50 and 70°C to form $\text{Os}_2(\text{CO})_6(\mu\text{-C}_6\text{H}_4\text{Ph})$ and $\text{Os}(\text{CO})_5$ by a bimolecular process, and reaction with PPh_3 at room temperature leads to similar fragmentation by what must also be a bimolecular reaction [6], CO dissociation requiring heat and being relatively slow [7]. Since it is known that clusters such as $\text{Fe}_3(\text{CO})_{12}$ also undergo ready fragmentation with larger nucleophiles but substitution with smaller ones [8] we have examined the reaction of **1** with a wide variety of P-donor ligands and find that stable mono substituted derivatives are formed with P-donors that have Tolman cone angles [9] as high as 143° . However, when the nucleophiles have cone angles $\geq 145^\circ$, it uniformly undergoes fragmentation to form mixtures of dinuclear and mononuclear osmium carbonyl complexes. The crystallographic structures of the clusters $\text{Os}_3(\text{CO})_8\text{L}(\mu\text{-C}_6\text{H}_4\text{Ph})$ (L = $\text{P}(\text{OCH}_2)_2\text{CF}_3$ (etpb) and $\text{P}(\text{OPh})_3$) have been determined.

2. Experimental and results

2.1. Chemicals

All P-donor ligands were obtained from commercial sources (Strem and Aldrich). Liquid phosphorus ligands

* Corresponding authors. A.J. Poë: tel.: +1-416-978 3924; fax: +1-416-978 3924; e-mail: apoe@alchemy.chem.utoronto.ca; D.H. Farrar: tel.: +1-416-978 3568; fax: +1-416-946 3303; e-mail: dfarrar@alchemy.chem.utoronto.ca

P(OMe)₃, P(OEt)₃, P(OMe)₂Ph, P(OEt)₂Ph, PMe₂Ph, PPh₂H, P(OPh)₃, P(O-i-Pr)₃, PEt₃, P(n-Pr)₃, P(n-Bu)₃, P(OMe)Ph₂, P(OEt)Ph₂, PMePh₂, PEtPh₂ and PCy₂H, were purified by distillation under reduced pressure of argon immediately before use. PPh₃ was recrystallized from ethanol. Etph was sublimed (50°C, reduced pressure) immediately before use. All the solvents for synthetic use were reagent grade. Heptane, hexane and pentane were dried and distilled over Na in the presence of benzophenone ketyl under an atmosphere of N₂. CH₂Cl₂ and acetonitrile were dried and distilled over CaH₂ under N₂. The solvents were bubbled with argon for 1 h after distillation and before use. All gases were obtained from Matheson or Canox Ltd. and were of Research Grade. Os₃(CO)₁₂ (Strem) and C₂Ph₂ (Aldrich) were used as received. Trimethylamine *N*-oxide (Aldrich) was sublimed prior to use and stored under dry argon. All manipulations were carried out by using standard Schlenk techniques under atmospheres of oxygen-free N₂ or Ar.

2.2. Synthesis of Os₃(CO)₉(μ-C₄Ph₄)

The violet cluster Os₃(CO)₉(μ-C₄Ph₄) (**1**) was prepared in crystalline form in 80% yield from Os₃(CO)₁₂ via Os₃(CO)₉(NCMe)(C₂Ph₂) by using the published method [10], and was purified by thin layer chromatography (TLC) (2:1 (vol./vol.) hexane–CH₂Cl₂). The IR spectrum of **1** in the C–O stretching region (Nicolet 5DX FT-IR spectrometer; in heptane: 2113.6 (s), 2057.5 (vs), 2042.8 (vs), 2035.3 (s, sh), 2011.9 (vs), 1998.2 (s), 1987.8 (m), 1930.2 (s) cm⁻¹) was in excellent agreement with that reported in decalin [6].

2.3. Syntheses of the clusters Os₃(CO)₈(etpb)(μ-C₄Ph₄)·(CH₃OH) (**2etpb**) and Os₃(CO)₈(P(OPh)₃)(μ-C₄Ph₄)·(C₆H₁₄) (**2P(OPH)₃**)

The monosubstituted complexes Os₃(CO)₈(etpb)(μ-C₄Ph₄) and Os₃(CO)₈(P(OPh)₃)(μ-C₄Ph₄) were obtained directly by CO substitution reactions of **1** (0.1 g, 0.087 mmol) with L (0.12 mmol) in heptane (20 cm³) and monitoring the FT-IR spectral changes until the ν(CO) bands of the parent compound had disappeared. The resulting solutions were evaporated under reduced pressure, and the residues dissolved in CH₂Cl₂ and purified by TLC (2:1 (vol./vol.) hexane–CH₂Cl₂). This afforded pink products in 90–95% yields and their ν(CO) stretching frequencies are listed in Table 1. Crystals of **2etpb** (Os₃(CO)₈(etpb)(μ-C₄Ph₄)·(CH₃OH)) were grown by slow evaporation of a CH₂Cl₂/CH₃OH solution of product, and crystals of **2P(OPH)₃** (Os₃(CO)₈(P(OPh)₃)(μ-C₄Ph₄)·(C₆H₁₄)) were grown by slow evaporation of a CH₂Cl₂/hexanes solution of product.

2.4. Crystallographic data collection, solution and refinement for Os₃(CO)₈(etpb)(μ-C₄Ph₄)·(CH₃OH) (**2etpb**) and Os₃(CO)₈(P(OPh)₃)(μ-C₄Ph₄)·(C₆H₁₄) (**2P(OPH)₃**)

Data for the crystal structure analyses of compounds **2etpb** and **2P(OPH)₃** are given in Table 2. A crystal of each compound was mounted on a glass fibre and accurate cell dimensions were determined on a CAD-4 diffractometer by a least squares treatment of the setting angles of 25 reflections in the range 12 < θ < 15°. ω-Scans of several intense low-angle

Table 1
C–O stretching frequencies for the clusters Os₃(CO)₈L(μ-C₄Ph₄)

L	χ ^a	θ (°) ^b	ν(CO) (cm ⁻¹) ^c						
Etph	31.20	101	2092.3 m	2047.9 vs	2023.8 s	2000.3 vs	1965.7 vs	1943.5 w	1916.1 m
P(OPh) ₃	30.20	128	2094.4 m	2049.6 vs	2017.8 s	1997.3 s	1965.2 vs	1930.0 w	1917.7 m
P(OMe) ₃	24.10	107	2083.2 m	2045.6 s	2013.4 vs	1993.0 s	1962.7 s	1942.6 w	1911.4 m
P(OEt) ₃	21.60	109	2082.0 m	2044.5 s	2011.7 vs	1991.6 s	1962.2 s	1937.3 m	1909.8 m
P(OMe) ₂ Ph	19.45	120	2080.9 m	2044.3 s	2011.3 vs	1992.8 s	1973.3 m	1960.9 s	1912.0 m
P(O-i-Pr) ₃	19.05	130	2080.2 m	2043.0 s	2009.8 vs	1990.4 s	1964.6 s	1942.2 w	1915.8 m
P(OEt) ₂ Ph	18.10	121	2080.5 m	2043.6 s	2010.0 vs	1991.3 s	1971.5 m	1959.0 s	1911.0 m
PPh ₂ H	17.35	126	2082.1 s	2050.7 vs	2014.2 vs	1994.0 s	1967.5 s	1953.9 m	1903.8 m
P(OMe)Ph ₂	16.30	132	2080.7 m	2050.9 s	2007.3 vs	1991.3 s	1967.7 m	1959.5 s	1919.6 m
P(OEt)Ph ₂	15.60	133	2080.2 m	2049.0 s	2006.2 vs	1991.0 s	1965.1 m	1958.2 s	1918.3 m
PMcPh ₂	12.10	136	2080.9 s	2051.1 vs	2007.0 vs	1992.2 vs	1967.6 s	1951.4 m	1901.4 m
PEtPh ₂	11.30	140	2081.0 m	2051.6 vs	2000.7 vs	1990.9 s	1967.6 s	1942.8 s	1889.5 m
PMe ₂ Ph	10.60	122	2078.6 m	2042.7 s	2004.3 vs	1991.4 s	1966.7 m	1949.7 s	1889.1 m
PCy ₂ H	9.10	143	2080.5 s	2048.4 vs	2015.6 m	1996.9 vs	1962.5 s	1956.2 s	1902.0 w
PEt ₃	6.30	132	2081.1 m	2050.2 vs	2014.4 s	1997.8 vs	1970.0 m	1943.5 s	1903.3 m
P(i-Pr) ₃	5.40	132	2081.6 m	2050.8 s	2016.9 vs	1999.2 vs	1966.8 s	1935.4 s	1902.4 m
P(n-Bu) ₃	5.25	132	2081.2 m	2051.1 s	2015.2 s	2000.1 vs	1975.6 m	1934.8 s	1901.9 m
PF ₃	54.7	104	2100 m	2058 vs	2018 s	2004 m	1976 s	1930 m	
				2036 vs			1992 s (sh)		

^a Ligand χ values (cm⁻¹) are taken from Ref. [23].

^b Tolman cone angles.

^c Spectra recorded in heptane, except for L = PF₃ [7].

Table 2
X-ray experimental data for **2etpb** and **2P(OPh)₃**

Compound	2etpb	2P(OPh)₃
Structural formula	Os ₃ (CO) ₉ (etpb)(μ-C ₆ H ₄) · (CH ₃ OH)	Os ₃ (CO) ₉ (P(OPh) ₃)(μ-C ₆ H ₄) · (C ₆ H ₁₄)
Empirical formula	C ₄₃ H ₃₅ O ₁₂ Os ₃ P	C ₄₃ H ₃₅ O ₁₂ Os ₃ P
<i>M</i>	1345	1548
Crystal system	triclinic	monoclinic
Space group	<i>P</i> $\bar{1}$ (No. 2)	<i>P</i> 2 ₁ / <i>n</i> (No. 14)
<i>a</i> (Å)	12.372(2)	11.939(2)
<i>b</i> (Å)	13.313(3)	27.591(6)
<i>c</i> (Å)	14.952(3)	17.209(3)
α (°)	96.64(3)	90
β (°)	103.05(3)	104.98(3)
γ (°)	106.77(3)	90
<i>U</i> (Å ³)	2253(1)	5476(3)
Crystal colour, habit, size (mm)	violet blocks, 0.20 × 0.25 × 0.18	violet blocks, 0.14 × 0.22 × 0.18
<i>Z</i>	2	4
<i>D_c</i> (g cm ⁻³)	1.98	1.88
<i>F</i> (000)	1264	2960
μ (Mo K α) (mm ⁻¹)	8.53	7.03
Indices	<i>h</i> - 14, 14; <i>k</i> - 15, 15; <i>l</i> 0, 17	<i>h</i> - 14, 13; <i>k</i> 0, 32; <i>l</i> 0, 20
2 θ Range (°)	1–50	1–50
No. data (<i>R_{int}</i>)	7801 (0.0163)	9952 (0.0412)
No. data used (criterion)	5143 (<i>F</i> > 4 σ (<i>F</i>))	6940 (<i>F</i> > 4 σ (<i>F</i>))
No. standards, frequency (h), decay (%)	3, 2, 0.03	3, 2, 0.01
Final <i>R</i> (<i>R_w</i>)	0.0388, (0.0452)	0.0465, (0.0858)
Number variables (obs./variables)	438 (11.7)	437 (15.9)
Largest (mean) final shift (e.s.d.)	0.03 (> 0.01)	0.01 (> 0.01)
Final density map (e Å ⁻³)	-0.99 to 1.13	-1.23 to 1.17
(Maximum near)	(Os(1))	(C(126))
Goodness-of-fit	1.26	2.53

reflections revealed that the crystal mosaicities were acceptable. The X-ray reflection data were measured at 23°C. The reflections measured were corrected for Lorentz and polarization effects. For **2etpb**, the space group *P* $\bar{1}$ was chosen based upon the cell parameters and the intensity distribution, and this space group was confirmed by a successful structure solution. The space group for **2P(OPh)₃**, *P*2₁/*n*, was determined from the systematic absences. The structures were solved by direct methods using the program SHELXTL PC [11].

For **2etpb**, a difference Fourier synthesis after location of the non-hydrogen atoms revealed the presence of electron density associated with a disordered phosphite ligand. The P atom and the carbon atom C16 are ordered; the disorder is associated with the -OCH₂- linkages. The major atom orientation, O(9a), O(10a) and O(11a) with site occupancy factors of 0.50, was located during the structure solution. Associated with each of the O atoms O(9a) and O(10a) are two other sites O(9b), O(9c), O(10b) and O(10c) with site occupancy factors of 0.25. The three partial O atoms labelled O(9) are bonded to C(13) which has a site occupancy factor of 1.0. The three partial O atoms labeled O(10) are bonded to C(14) which has a site occupancy factor of 1.0. The third -OCH₂- group is disordered over two sites O(11a)-C(15a) and O(11b)-C(15b) each with a site occupancy factor of 0.5. A diagram depicting the disorder model is available with supplementary material. At this stage, two additional peaks,

separated from the Os₃ cluster, were noted in a difference Fourier synthesis. These peaks were assigned to the C and O atoms of a CH₃OH solvent molecule. The atoms refined with an occupancy factor of 1.0. The H-atoms associated with the CH₃OH solvent molecule could not be located in a difference Fourier synthesis and were not included in the model. H atoms associated with the phenyl rings, the methylene groups and the methyl group were positioned on geometric grounds and included (as riding atoms) in the structure factor calculation (*U*_{iso} - sp² refined to 0.17 Å² and *U*_{iso} - sp³ refined to 0.32 Å²). Refinement was by full-matrix least-squares calculations on *F* using the weighting scheme $w^{-1} = \sigma^2(F) + 0.0005F^2$. Anisotropic thermal parameters were refined for all non-H atoms except the phenyl ring C atoms and the O atom associated with the minor orientation of the phosphite ligand which were refined with isotropic thermal parameters. Data were corrected for absorption effects by a semi-empirical method using the program SHELXA [12]. Correction factors ranged from 0.270 to 0.541. No correction was made for secondary extinction. The atomic coordinates are given in Table 3. Selected bond lengths and angles for **2etpb** are listed in Table 4. An ORTEP [13] view of the molecule is presented in Fig. 1. Scattering factors for neutral atoms were used in the refinement [14].

For **2P(OPh)₃**, a difference Fourier synthesis after location of the Os₃ cluster non-hydrogen atoms revealed the presence of a n-hexane solvent molecule. Initial attempts to refine the

Table 3

Atomic coordinates ($\times 10^{-4}$) and equivalent isotropic displacement coefficients ($\text{\AA}^2 \times 10^{-3}$) for **2etpb**

Atoms	x	y	z	U_{eq}^a
Os(1)	2734(1)	3276(1)	3675(1)	47(1)
Os(2)	1596(1)	1953(1)	1957(1)	42(1)
Os(3)	2879(1)	4000(1)	1933(1)	51(1)
C(1)	2455(12)	4629(10)	3908(10)	70(6)
O(1)	2277(10)	5404(8)	4084(7)	93(6)
C(2)	2816(11)	3061(10)	4909(9)	64(6)
O(2)	2906(10)	2910(10)	5657(7)	105(6)
C(3)	4417(12)	3948(10)	3935(8)	61(6)
O(3)	5398(9)	4322(9)	4109(7)	98(5)
C(4)	2128(11)	1339(10)	1024(9)	60(6)
O(4)	2449(9)	976(8)	450(6)	89(5)
C(5)	307(12)	1928(11)	980(10)	69(7)
O(5)	-481(9)	1881(10)	404(7)	105(6)
C(6)	4169(12)	3430(10)	1923(9)	59(6)
O(6)	4894(9)	3115(8)	1855(7)	87(5)
C(7)	3869(13)	5447(12)	2324(10)	76(7)
O(7)	4496(11)	6295(8)	2577(9)	120(6)
C(8)	1426(13)	4281(10)	1908(9)	68(6)
O(8)	579(10)	4472(9)	1853(8)	102(6)
C(9)	2788(9)	1711(8)	3248(8)	45(4)
C(10)	1718(10)	879(8)	3023(7)	45(5)
C(11)	694(9)	1197(8)	3001(7)	45(5)
C(12)	908(9)	2331(9)	3218(7)	46(5)
C(91)	3902(11)	1433(9)	3448(8)	58(3)
C(92)	4334(11)	1033(10)	2782(9)	65(3)
C(93)	5372(13)	757(12)	3056(11)	85(4)
C(94)	5927(15)	878(13)	3951(12)	100(5)
C(95)	5519(17)	1262(14)	4660(14)	121(6)
C(96)	4509(15)	1578(13)	4400(12)	106(5)
C(101)	1628(10)	-283(9)	2899(8)	51(3)
C(102)	1722(13)	-740(12)	3667(11)	84(4)
C(103)	1747(15)	-1814(14)	3586(12)	106(5)
C(104)	1648(13)	-2356(12)	2745(11)	88(4)
C(105)	1457(15)	-1977(14)	1983(12)	105(5)
C(106)	1462(12)	-899(11)	2047(10)	76(4)
C(111)	-507(9)	393(8)	2855(7)	45(3)
C(112)	-1246(11)	-118(10)	1990(8)	58(3)
C(113)	-2339(12)	-827(11)	1916(10)	77(4)
C(114)	-2679(12)	-1062(11)	2695(10)	74(4)
C(115)	-1949(13)	-582(11)	3563(10)	77(4)
C(116)	-846(12)	175(10)	3663(9)	70(4)
C(121)	-83(10)	2719(9)	3320(8)	48(3)
C(122)	-1092(10)	2507(9)	2616(9)	60(3)
C(123)	-2028(12)	2796(10)	2794(9)	71(4)
C(124)	-1986(13)	3248(11)	3641(10)	81(4)
C(125)	-997(13)	3520(11)	4350(10)	81(4)
C(126)	8(11)	3246(10)	4197(9)	65(3)
P	2642(3)	4117(3)	421(2)	59(1)
O(9A)	1816(21)	3049(17)	-318(16)	62(11)
O(9B)	1477(38)	3262(36)	-285(30)	46(13)
O(9C)	2427(29)	3140(26)	-281(22)	35(9)
O(10A)	3727(19)	3992(24)	-7(14)	88(13)
O(10B)	3774(36)	4627(37)	143(29)	43(10)
O(10C)	3639(43)	5021(40)	234(30)	72(15)
O(11A)	2436(36)	5111(21)	101(18)	110(22)
O(11B)	1683(29)	4649(27)	41(27)	119(19)
C(13)	1697(23)	3219(14)	-1280(11)	153(14)
C(14)	3620(21)	4435(38)	-905(15)	338(34)
C(15A)	2355(59)	5182(33)	-912(26)	130(37)
C(15B)	1526(43)	4702(46)	-936(33)	129(29)

(continued)

Table 3 (continued)

Atoms	x	y	z	U_{eq}^a
C(16)	2397(18)	4277(15)	-1363(11)	96(9)
C(17)	2366(18)	4394(19)	-2395(13)	140(12)
C(18)	1337(23)	4130(18)	-2964(15)	178(18)
O(20)	4311(26)	9182(23)	39(22)	365(17)
C(20)	3820(33)	8002(30)	555(26)	264(16)

^a Equivalent isotropic U defined as one third of the trace of the orthogonalized U_{ij} tensor.

Table 4

Selected bond lengths (\AA) and angles ($^\circ$) for **2etpb** and **2P(OPh)₃**

	2etpb	2P(OPh)₃
Os(1)–Os(2)	2.752(1)	2.760(1)
Os(1)–Os(3)	2.904(1)	2.921(1)
Os(2)–Os(3)	2.738(1)	2.732(1)
Os(1)–C(9)	2.13(1)	2.18(2)
Os(1)–C(12)	2.15(1)	2.05(1)
Os(2)–C(9)	2.27(1)	2.30(2)
Os(2)–C(10)	2.27(1)	2.24(2)
Os(2)–C(11)	2.28(1)	2.31(2)
Os(2)–C(12)	2.30(1)	2.27(2)
Os(3)–P	2.244(4)	2.261(5)
Os(2)–Os(1)–Os(3)	57.8(1)	57.4(1)
Os(1)–Os(2)–Os(3)	63.9(1)	64.3(1)
Os(1)–Os(3)–Os(2)	58.3(1)	58.3(1)
Os(2)–Os(1)–C(9)	53.5(3)	54.0(5)
Os(3)–Os(1)–C(9)	96.8(3)	99.1(5)
Os(2)–Os(1)–C(12)	54.3(3)	53.9(5)
Os(3)–Os(1)–C(12)	96.9(3)	94.5(5)
C(9)–Os(1)–C(12)	77.4(4)	76.6(6)
Os(1)–C(9)–Os(2)	77.4(4)	75.9(6)
Os(1)–C(9)–C(10)	116.1(9)	115.9(15)
Os(2)–C(9)–C(10)	72.2(6)	71.2(12)
Os(1)–C(9)–C(91)	123.0(6)	120.3(10)
Os(2)–C(9)–C(91)	135.0(9)	129.9(12)
C(10)–C(9)–C(91)	118.3(10)	123.2(18)
Os(2)–C(10)–C(9)	71.9(7)	76.4(12)
Os(2)–C(10)–C(11)	71.9(7)	73.1(10)
C(9)–C(10)–C(11)	115.9(10)	121.7(19)
Os(2)–C(10)–C(101)	130.6(8)	127.8(13)
C(9)–C(10)–C(101)	123.1(11)	129.7(19)
C(11)–C(10)–C(101)	120.8(9)	108.2(14)
Os(2)–C(11)–C(10)	71.1(7)	68.2(10)
Os(2)–C(11)–C(12)	72.4(7)	69.3(9)
C(10)–C(11)–C(12)	115.6(9)	106.2(14)
Os(2)–C(11)–C(111)	130.9(7)	135.9(13)
C(10)–C(11)–C(111)	122.2(10)	124.9(17)
C(12)–C(11)–C(111)	122.0(11)	127.9(18)
Os(1)–C(12)–Os(2)	76.4(4)	79.1(6)
Os(1)–C(12)–C(11)	114.1(8)	119.0(13)
Os(2)–C(12)–C(11)	70.9(7)	72.0(10)
Os(1)–C(12)–C(121)	125.5(7)	126.1(11)
Os(2)–C(12)–C(121)	132.7(8)	129.5(12)
C(11)–C(12)–C(121)	118.8(9)	113.6(14)

positional parameters of the solvent C atoms led to an unacceptable geometry for the hexane molecule. The hexane molecule was successfully refined by applying distance constraints to the C–C bonds and to the 1–3 non-bonded C...C

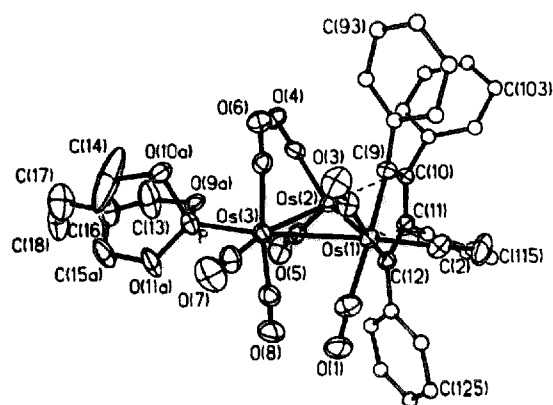


Fig. 1. A view of the molecule $\text{Os}_3(\text{CO})_9(\text{etpb})(\mu\text{-C}_6\text{Ph}_3)$ (**2etpb**) with 25% probability ellipsoids. H atoms are omitted, for clarity.

distances. H atoms associated with the phenyl rings, and the methylene and methyl groups were positioned on geometric grounds and included (as riding atoms) in the structure factor calculation ($U_{\text{iso}} - sp^2$ refined to 0.18 \AA^2 and $U_{\text{iso}} - sp^3$ was fixed as 0.15 \AA^2). Refinement was by full-matrix least-squares calculations on F using the weighting scheme $w^{-1} = \sigma^2(F) + 0.0005F^2$. Anisotropic thermal parameters were refined for all non-H atoms except the phenyl ring C atoms which were refined with isotropic thermal parameters. Data were corrected for absorption effects by a semi-empirical method using the program SHELXA [12]. Correction factors ranged from 0.370 to 0.600. No correction was made for secondary extinction. The atomic coordinates are given

Table 5
Atomic coordinates ($\times 10^{-4}$) and equivalent isotropic displacement coefficients ($\text{\AA}^2 \times 10^{-3}$) for **2P(OPh)₃**

Atoms	<i>x</i>	<i>y</i>	<i>z</i>	U_{eq}^a
Os(1)	628(1)	671(1)	1206(1)	30(1)
Os(2)	1238(1)	1424(1)	2290(1)	28(1)
Os(3)	134(1)	1684(1)	751(1)	30(1)
C(1)	1055(15)	700(7)	187(10)	39(7)
O(1)	1330(11)	674(5)	-383(7)	54(6)
C(2)	952(15)	-5(7)	1378(10)	37(7)
O(2)	1116(13)	-404(6)	1440(9)	67(7)
C(3)	-934(18)	593(7)	665(11)	45(8)
O(3)	-1956(12)	530(6)	233(9)	68(6)
C(4)	239(24)	1831(7)	2672(14)	70(11)
O(4)	-366(14)	2064(5)	2947(9)	69(7)
C(5)	2293(14)	1937(7)	2448(10)	40(7)
O(5)	2900(12)	2252(6)	3502(10)	69(6)
C(6)	-1284(16)	1575(7)	1099(12)	42(7)
O(6)	-2089(11)	1514(6)	1331(9)	59(6)
C(7)	-595(16)	1657(7)	-334(10)	44(7)
O(7)	-1061(16)	1604(6)	-1005(10)	81(8)
C(8)	1660(14)	1729(7)	607(10)	35(6)
O(8)	2550(12)	1771(6)	486(9)	60(6)
C(9)	366(14)	694(6)	2414(10)	33(6)
C(10)	1276(17)	735(7)	2986(11)	44(7)
C(11)	2458(17)	792(6)	2833(11)	41(7)
C(12)	2259(14)	809(6)	1924(10)	32(6)

(continued)

Table 5 (continued)

Atoms	<i>x</i>	<i>y</i>	<i>z</i>	U_{eq}^a
C(91)	-813(15)	590(7)	2544(10)	38(4)
C(92)	-1229(18)	874(8)	3083(12)	59(6)
C(93)	-2434(18)	742(8)	3120(12)	58(6)
C(94)	-2916(18)	356(8)	2834(12)	56(6)
C(95)	-2481(19)	70(9)	2334(12)	61(6)
C(96)	-1404(16)	180(7)	2183(11)	48(5)
C(101)	1443(16)	675(7)	3931(11)	40(4)
C(102)	1371(16)	217(8)	4185(11)	50(5)
C(103)	1456(20)	138(10)	4985(14)	75(7)
C(104)	1448(22)	505(11)	5475(16)	85(8)
C(105)	1421(21)	977(10)	5188(15)	77(7)
C(106)	1450(16)	1051(7)	4410(11)	46(5)
C(111)	3499(13)	744(6)	3409(9)	26(4)
C(112)	4007(18)	1136(8)	3971(12)	55(5)
C(113)	4999(19)	1035(8)	4550(12)	58(6)
C(114)	5505(20)	610(9)	4556(14)	64(6)
C(115)	5123(17)	254(8)	4109(12)	51(5)
C(116)	4050(18)	292(8)	3496(12)	58(6)
C(121)	3356(15)	826(7)	1657(10)	38(4)
C(122)	4258(16)	1169(7)	1919(11)	46(5)
C(123)	5206(17)	1165(8)	1602(11)	52(5)
C(124)	5419(19)	815(9)	1123(13)	66(6)
C(125)	4544(25)	420(11)	864(17)	97(9)
C(126)	3464(19)	460(9)	1111(13)	64(6)
P	-24(4)	2501(2)	749(3)	34(2)
O(9)	130(12)	2707(4)	1611(7)	46(5)
C(21)	290(18)	3208(8)	1881(12)	54(5)
C(22)	1087(17)	3288(8)	2504(12)	51(5)
C(23)	1224(24)	3768(10)	2864(16)	89(8)
C(24)	427(25)	4108(12)	2492(17)	94(9)
C(25)	-409(20)	4020(9)	1853(14)	68(6)
C(26)	-586(19)	3537(8)	1495(13)	57(6)
O(10)	-1196(10)	2737(5)	209(7)	43(5)
C(31)	-2298(15)	2594(7)	240(10)	40(4)
C(32)	-2680(19)	2616(8)	913(13)	58(6)
C(33)	-3760(21)	2490(9)	923(14)	73(7)
C(34)	-4493(21)	2283(9)	240(14)	74(7)
C(35)	-4065(22)	2230(10)	-440(15)	76(7)
C(36)	-3006(19)	2373(8)	-486(13)	62(6)
O(11)	878(10)	2821(5)	442(7)	41(5)
C(41)	1193(14)	2816(6)	-269(10)	32(4)
C(42)	471(17)	2720(7)	-991(11)	48(5)
C(43)	778(20)	2757(9)	-1723(14)	67(6)
C(44)	2046(21)	2853(9)	-1591(14)	71(7)
C(45)	2672(22)	2907(9)	-932(14)	70(7)
C(46)	2349(20)	2872(9)	-223(14)	65(6)
C(51)	3149(38)	1379(17)	8574(26)	232(24)
C(52)	2071(37)	1567(18)	8073(29)	246(27)
C(53)	1520(38)	1316(23)	7375(27)	371(46)
C(54)	328(38)	1218(19)	7425(32)	309(35)
C(55)	-539(38)	1446(16)	6851(32)	244(27)
C(56)	-1563(36)	1089(15)	6535(26)	241(25)

^a Equivalent isotropic U defined as one third of the trace of the orthogonalized U_{ij} tensor.

in Table 5 and selected bond lengths and angles for **2P(OPh)₃** are listed in Table 4. An ORTEP view of the molecule is presented in Fig. 2; the same atom labelling scheme was used for both structures. A diagram showing the hexane solvent molecule is available with supplementary material.

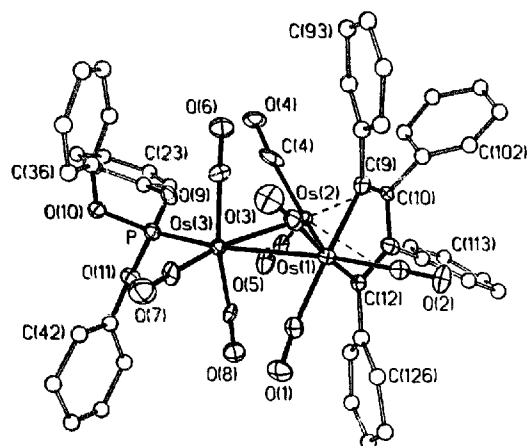


Fig. 2. A view of the molecule $\text{Os}_3(\text{CO})_8(\text{P}(\text{OPh})_3)(\mu\text{-C}_4\text{Ph}_4)$ ($2\text{P}(\text{OPh})_3$) with 25% probability ellipsoids. H atoms are omitted, for clarity.

2.5. Reactions of $\text{Os}_3(\text{CO})_6(\mu\text{-C}_4\text{Ph}_4)$ with other P-donors of cone angle $\leq 143^\circ$

The cluster **1** was reacted with a large variety of smaller P-donor ligands L ($\text{L} = \text{P}(\text{OMe})_3$, $\text{P}(\text{OEt})_3$, $\text{P}(\text{OMe})_2\text{Ph}$, $\text{P}(\text{OEt})_2\text{Ph}$, PMe_2Ph , PPh_2H , $\text{P}(\text{O-i-Pr})_3$, PEt_3 , $\text{P}(\text{n-Pr})_3$, $\text{P}(\text{n-Bu})_3$, $\text{P}(\text{OMe})\text{Ph}_2$, $\text{P}(\text{OEt})\text{Ph}_2$, PMePh_2 , PEtPh_2 and PCy_2H ; listed in ascending order of cone angles and with the largest cone angle being 143°) in exactly the same way as for the syntheses of **2etpb** and **2P(OPh)₃**, and the products isolated also as before. The $\nu(\text{CO})$ stretching frequencies are listed in Table 1.

The reactions with all these smaller P-donor ligands proceeded in two observable stages. With a ten-fold excess and quite large absolute concentrations of the ligands the initial violet color of **1** was immediately replaced by a yellow color which changed over the next few minutes to the pink-violet color characteristic of the products. When the concentrations of the ligands were reduced to one molar equivalent the initial color changes occurred over a period of 1–2 min, but the subsequent changes occurred at roughly the same rates as before.

2.6. Reactions of $\text{Os}_3(\text{CO})_6(\mu\text{-C}_4\text{Ph}_4)$ with larger P-donors of cone angle $\geq 145^\circ$

The larger ligands $(p\text{-XC}_6\text{H}_4)_3\text{P}$ ($\text{X} = \text{F}, \text{C}, \text{Cl}, \text{F}$ and H) and $\text{P}(\text{NMe}_2)_3$ (all with cone angles $\geq 145^\circ$) react in only one observable step (even at low values of $[\text{L}]$) at rates clearly dependent on $[\text{L}]$, to form mixtures of mono- and dinuclear osmium carbonyls. Thus the mixture of products of reaction with PPh_3 were separated by TLC (2:1 (vol./vol.) hexane- CH_2Cl_2) into two pairs of components: (a) $\text{Os}(\text{CO})_3(\text{PPh}_3)_2$ ($\nu(\text{CO}) = 890 \text{ cm}^{-1}$) [15] and $\text{Os}_2(\text{CO})_6(\mu\text{-C}_4\text{Ph}_4)$ ($\nu(\text{CO}) = 2081$ (s), 2051 (vs), 2015 (m), 1998 (s) and 1972 (m) cm^{-1}) [16], and (b) $\text{Os}(\text{CO})_4\text{PPh}_3$ ($\nu(\text{CO}) = 2060$ (s), 1980 (m) and 1943

(vs) cm^{-1}) [11] and $\text{Os}_2(\text{CO})_5(\text{PPh}_3)(\mu\text{-C}_4\text{Ph}_4)$ ($\nu(\text{CO}) = 2057$ (s), 2005 (vs) and 1929 (m) cm^{-1}), all the spectra being measured in CH_2Cl_2 . The assignment of the last group of IR bands to $\text{Os}_2(\text{CO})_5(\text{PPh}_3)(\mu\text{-C}_4\text{Ph}_4)$ is proposed so that the number of CO ligands in this pair of products is the same as in the reactant cluster. This assumption is supported by the cleanness of the reactions as evidenced by the presence of isosbestic points in the successive spectra taken during the course of the reactions. The products of reactions with the other larger ligands listed above were not separated but the changing FT-IR spectra in heptane were monitored throughout the course of the reactions. The bands due to $\text{Os}_2(\text{CO})_6(\mu\text{-C}_4\text{Ph}_4)$ were observed in all cases except for $\text{L} = \text{P}(\text{NMe}_2)_3$, when only its lowest frequency band at 2081 cm^{-1} was clearly distinguishable. Bands assignable to $\text{Os}(\text{CO})_3\text{L}_2$ at 1881 ($\text{P}(\text{NMe}_2)_3$), 1900 (PPh_3), 1896 ($\text{P}(p\text{-FC}_6\text{H}_4)_3$), 1900 ($\text{P}(p\text{-ClC}_6\text{H}_4)_3$), and 1903 ($\text{P}(p\text{-F}_3\text{CC}_6\text{H}_4)_3$) cm^{-1} were observed and three matching bands assignable to $\text{Os}(\text{CO})_4\text{L}$ were observed for $\text{L} = \text{P}(\text{NMe}_2)_3$, PPh_3 and $\text{P}(p\text{-FC}_6\text{H}_4)_3$. Only the lower frequency bands at $\sim 1930\text{--}1940 \text{ cm}^{-1}$ were observed for $\text{Os}(\text{CO})_4\text{L}$ when $\text{L} = \text{P}(p\text{-ClC}_6\text{H}_4)_3$ and $\text{P}(p\text{-F}_3\text{CC}_6\text{H}_4)_3$.

The ratios of the intensities of the bands at 2081 and/or 2051 cm^{-1} (due to $\text{Os}_2(\text{CO})_6(\mu\text{-C}_4\text{Ph}_4)$) to those of the bands at $\sim 1900 \text{ cm}^{-1}$ due to the $\text{Os}(\text{CO})_3\text{L}_2$ complexes is approximately constant. This is in contrast to the ratios of the intensities of the bands due to $\text{Os}(\text{CO})_4\text{L}$ at $\sim 1930\text{--}1940 \text{ cm}^{-1}$ to those due to $\text{Os}(\text{CO})_3\text{L}_2$ at $\sim 1890\text{--}1900 \text{ cm}^{-1}$ which vary from $\sim 0.6:1$ to $6:1$ as the basicity of the ligands increases [9] along the series $\text{P}(p\text{-XC}_6\text{H}_4)_3$ ($\text{X} = \text{CF}_3, \text{Cl}, \text{F}, \text{H}$) and $\text{P}(\text{NMe}_2)_3$. Provided the intensities of the carbonyls $\text{Os}(\text{CO})_3\text{L}_2$ are not too dependent on the basicity of the substituents we can therefore conclude that the carbonyls $\text{Os}(\text{CO})_3\text{L}_2$ and $\text{Os}_2(\text{CO})_6(\mu\text{-C}_4\text{Ph}_4)$ are formed together as one pair of products, and that $\text{Os}(\text{CO})_4\text{L}$ and the putative $\text{Os}_3(\text{CO})_5\text{L}(\mu\text{-C}_4\text{Ph}_4)$ are formed together as another pair. The ratio of the yields of $\text{Os}(\text{CO})_4\text{L}$ to those of the corresponding $\text{Os}(\text{CO})_3\text{L}_2$ and $\text{Os}_2(\text{CO})_6(\mu\text{-C}_4\text{Ph}_4)$ pairs increases substantially with the basicities of the substituents. The fact that not all bands due to the various products can be seen in all cases arises from the changing relative intensities of the pairs of products and the consequent overlap of some bands.

3. Discussion

The final products of the reactions of **1** with **etpb** and **P(OPh)₃** are clearly the clusters $\text{Os}_3(\text{CO})_8\text{L}(\mu\text{-C}_4\text{Ph}_4)$ (**2**) in which the substitutions have occurred at the $\text{Os}(\text{CO})_4$ moiety in the parent cluster and the substituent is essentially *trans* to the Os atom that is in the osmacyclopentadiene ring.

The main structural features of the clusters **2etpb** and **2P(OPh)₃** are similar to those in the parent cluster **1** [1]. Two of the four coordination sites on atoms Os(2) are occupied by π -bonds from an osmacyclopentadiene ligand. In the

structures of **2etbp**, **2P(OPh)₃** and the parent cluster **1**, the Os–Os bonds involving Os(2) are significantly shorter than the average Os–Os distance in Os₃(CO)₁₂ of 2.844(5) Å [17]. The Os(1)–Os(3) distances, 2.904(1) and 2.921(1) Å for **2etbp** and **2P(OPh)₃**, respectively, are significantly longer than the Os₃(CO)₁₂ distances and in the range of the values 2.917(2) and 2.894(1) Å reported for **1**. (The structure of **1** has been determined in a monoclinic and an orthorhombic form.) Thus the phosphite ligands have very little effect upon the geometrical parameters of the Os₃ core. The structure of the closely related cluster Os₃(CO)₉{C(SiMe₃)CMeCHCPh} is quite different. It contains an osmacyclopentadiene ligand with a π-bond to each of the two Os atoms not in the osmacyclopentadiene ring [18]. In this cluster the Os–Os distances that involve the Os atom in the ring and an Os atom with a π-bond are both 2.811(1) Å. The Os–Os distance between the two Os atoms with π-bonds is 2.825(1) Å.

All other geometrical parameters associated with the structures **2etbp** and **2P(OPh)₃** are in the ranges observed in the parent cluster **1** [1] and, where comparable, in Os₃(CO)₉{C(SiMe₃)CMeCHCPh} [18].

Since the C–O stretching frequencies in Table 1 show little dependence on the nature of the substituents it can be concluded that all the clusters have the same structures and, particularly, that no multiple substitutions had occurred. The most likely ligands to produce multisubstitutions are the small phosphites **etpb**, **P(OMe)₃** and **P(OEt)₃** [19] but there is no spectroscopic or crystallographic evidence for that and solutions of all the products were stable in the presence of excess ligand for months at ambient temperatures. This is corroborated by the observation that the violet cluster Os₃(CO)_n(PF₃)₃(μ-C₄Ph₄) can be synthesized by addition of PF₃ to the unusual unsaturated cluster Os₃(CO)_n(μ-C₄Ph₄) [7]. Further reaction with an excess of PF₃ proceeds very slowly even though multisubstitution reactions by PF₃ are well known due to its very high π bonding ability. The monosubstituted cluster was characterized by its mass and NMR spectra [7] and, since PF₃ (θ = 104°) falls into the group of 'small' ligands as defined here, its C–O stretching frequencies are included in Table 1. It is also clear that the effects of the different substituents on the C–O stretching frequencies are dissipated widely over the whole cluster, no localized effect of the sort that could be associated with changing substituent basicity being apparent.

Reactions of **1** with the group of larger ligands (θ ≥ 145°) are evidently very different. With L = PPh₃ the known com-

plexes Os(CO)₃L₂, Os(CO)₄L and Os₂(CO)₆(μ-C₄Ph₄) were isolated from the product mixture and characterized spectroscopically. The fourth product isolated was not characterized other than by measurement of its C–O stretching frequencies and its assignment to Os₂(CO)₅PPh₃(μ-C₄Ph₄) is based more on the cleanness of the reactions and the stoichiometric symmetry that its existence would provide. Attempts to obtain crystals suitable for structure determination were unfortunately not successful. In spite of this gap in our knowledge, the products Os(CO)₃L₂ and Os₂(CO)₆(μ-C₄Ph₄) do seem to be formed in equimolar amounts that are clearly different from the yields of Os(CO)₄L and what we assume to be Os₂(CO)₅(PPh₃)(μ-C₄Ph₄). The relative yields of Os(CO)₃L₂ and the pair of products Os₂(CO)₆(μ-C₄Ph₄) and Os(CO)₄L are very dependent on the nature of the ligands, those of Os(CO)₃L₂ becoming relatively much greater with increasing ligand basicity.

Some of the important features of the reactions observed here are reminiscent of the behavior of the clusters M₅C(CO)₁₅ (M = Ru and Fe) [20,21]. The color changes and relative rates of the reactions with smaller ligands all suggest initial formation of cluster-ligand adducts in a bimolecular process that is accompanied, in the case of the M₅C clusters, by the opening up of the clusters with major changes in the electronic spectra. This is followed by dissociative loss of CO and reversion to the closed form of the now substituted clusters which have colors similar to those of the unsubstituted ones. When M = Ru this substitution path is only observed for ligands with cone angles of ≤ 133°, those with cone angles of ≥ 136° leading to monosubstituted products by a single and quite different path [20]. When M = Fe, ligands with θ ≤ 128° lead to monosubstitution via reversible bimolecular adduct formation followed by CO dissociation but, when θ ≥ 136°, fragmentation or decomposition occurs [21]. These very small cone angle gaps between ligands that produce the same or different products by quite different paths are quite remarkable but the steric effects are accompanied by changes in ligand basicity and it is likely that electronic effects also contribute to the different behavior. In general the smallest of the larger ligands involved are of substantially lower basicity than the largest of the smaller ligands [20,21]. In the reactions reported here, the smaller ligands also lead to substitution, most probably via associative adduct formation, while the larger ligands lead to fragmentation products via F_N2 [22] processes. The cone angle gap of 2° between the largest small ligand, PCy₂H, and the smallest large ligands, P(*p*-XC₆H₄)₃, is not, of course very precisely defined because the cone angle of the former is itself not precisely defined either. The distinction between the reactions involving smaller and larger ligands is clearly reflected in the nature of the products as well as in the number of observable steps. More detailed kinetic and other studies would be required to establish possible reasons for this type of behavior.

¹ It has also been reported [7] that Os₃(CO)_n(PPh₃)₃(μ-C₄Ph₄) can be synthesized by addition of PPh₃ to Os₃(CO)_n(μ-C₄Ph₄). It has C–O stretching frequencies in quite good accord with those of the other Os₃(CO)_nL₃(μ-C₄Ph₄) clusters but it is black-green and no mass spectrum could be obtained. This suggests that, if it is thermodynamically stable enough to be isolated, its Os₃ cluster must be sufficiently distorted to alter its color significantly and it cannot be as stable as the other monosubstituted clusters. Nevertheless, the failure to prepare it by direct substitution of PPh₃ into Os₃(CO)_n(μ-C₄Ph₄) would be for kinetic and not thermodynamic reasons.

4. Supplementary material

Tables and diagrams of complete molecular geometries, anisotropic displacement coefficients, H atom coordinates (9 pages for **2etbp** and 8 pages for **2P(OPh)₃**) and tables of structure factors (17 pages for **2etbp** and 22 pages for **2P(OPh)₃**) are available from author D.H.F.

Acknowledgements

The support of the Natural Science and Engineering Research Council, Ottawa, is gratefully acknowledged, as is The Ministry of Education and Science, Madrid, for the award of a fellowship (to C.M.) to enable her to visit the University of Toronto and carry out the work described here.

References

- [1] G. Ferraris and G. Gervasio, *J. Chem. Soc., Dalton Trans.*, (1974) 1813.
- [2] R.D. Adams and P. Selegue, in G. Wilkinson, F.G.A. Stone and E.W. Abel (eds.), *Comprehensive Organometallic Chemistry*, Vol. 4, Pergamon, Oxford, 1982, Ch. 33, p. 1033.
- [3] G.A. Vaglio, O. Gambino, R.P. Ferrari and G. Cetini, *Inorg. Chim. Acta*, 7 (1973) 193.
- [4] A.K. Smith, in G. Wilkinson, F.G.A. Stone and E.W. Abel (eds.), *Comprehensive Organometallic Chemistry II*, Vol. 7, Pergamon, Oxford, 1995, Ch. 13; G. Lavigne, in D.F. Shriver, H.D. Kaesz and R.D. Adams (eds.), *The Chemistry of Metal Cluster Complexes*, VCH, New York, 1990, Ch. 5; A.J. Deeming, in B.F.G. Johnson (ed.), *Transition Metal Clusters*, Wiley, Chichester, 1980, Ch. 6.
- [5] J.A. Connor, *Top. Curr. Chem.*, 71 (1977) 71.
- [6] A.J. Poë, C.N. Sampson and R.T. Smith, *J. Am. Chem. Soc.*, 108 (1986) 5459.
- [7] R.P. Ferrari, G.A. Vaglio, O. Gambino, M. Valle and G. Cetini, *J. Chem. Soc., Dalton Trans.*, (1972) 1998.
- [8] S.M. Grant and A.R. Manning, *Inorg. Chim. Acta*, 31 (1978) 41.
- [9] C.A. Tolman, *Chem. Rev.*, 77 (1977) 313.
- [10] M.A. Gallop, B.F.G. Johnson, R.K. Khattar, J. Lewis and P.R. Raithby, *J. Organomet. Chem.*, 386 (1990) 121.
- [11] SHELXTL PC, Version 4.1, Siemens Analytical Instruments, Madison, WI, 1990.
- [12] G.M. Sheldrick, SHELXA-90, semi-empirical absorption correction, Version 1.0, University of Göttingen, Göttingen, Germany, 1990.
- [13] C.K. Johnson, ORTEPII, Rep. ORNL-5138, Oak Ridge National Laboratory, Oak Ridge, TN, 1976.
- [14] *International Table of Crystallography*, Vol. 4, Kynoch Press, Birmingham, UK, 1969.
- [15] F. L'Eplattenier and F. Calderazzo, *Inorg. Chem.*, 7 (1968) 1290.
- [16] O. Gambino, G.A. Vaglio, R.P. Ferrari and G. Cetini, *J. Organomet. Chem.*, 30 (1971) 381.
- [17] M.R. Churchill and B.G. DeDoer, *Inorg. Chem.*, 16 (1977) 878.
- [18] A.A. Kordze, N.M. Astakhova, F.M. Dolgushin, A.I. Yanovsky, Y.T. Struchkov and P.V. Petrovskii, *Organometallics*, 14 (1995) 2167.
- [19] C.A. Tolman, *J. Am. Chem. Soc.*, 92 (1970) 2956.
- [20] D.H. Farrar, A.J. Poë and Y. Zheng, *J. Am. Chem. Soc.*, 116 (1994) 6252.
- [21] A.J. Poë and Y. Zheng, *Inorg. Chim. Acta*, 252 (1996) 311.
- [22] N. Brodie, A.J. Poë and V. Sekhar, *J. Chem. Soc., Chem. Commun.*, (1985) 1090; A.J. Poë and V.C. Sekhar, *Inorg. Chem.*, 24 (1985) 4376.
- [23] T. Bartik, T. Himmler, H.-G. Schulte and K. Seevogel, *J. Organomet. Chem.*, 272 (1984) 29.